Liquefaction-Induced Ground and Building Interactions in İskenderun from the 2023 Kahramanmaraş Earthquake Sequence

Diane M. Moug,^{a)} M.EERI, Jonathan D. Bray,^{b)} M.EERI, Patrick Bassal,^{c)} M.EERI, Jorge Macedo,^{d)} Kristin Ulmer,^{e)} K. Önder Cetin^{f)}, Sena Begüm Kendır,^{g)} Arda Şahin^{h)}, Cody Arnold^{d)}, Murat Bikçeⁱ⁾

Significant and widespread liquefaction occurred in İskenderun during the 2023 M_w 7.8 Kahramanmaraş earthquake. Liquefaction effects on buildings were observed in several areas of Iskenderun, predominantly in areas of reclaimed land and near historic shorelines. Liquefaction-induced building settlements were particularly concentrated in the Çay District, which is almost entirely reclaimed land. Liquefaction-induced ground and building settlements were either marginal or not apparent in areas away from the historical shorelines. Building settlement and ground deformation were documented at 26 buildings in Iskenderun through lidar scans and laserlevel hand measurements. Liquefaction-induced building settlements ranged from 0 to 740 mm. Building-ground interactions were evident from hogging ground deformations, including cases where buildings deformed nearby ground and damaged nearby buildings, and sagging buildings. Historic land development affected the spatial extent of observed liquefaction-induced building damage. Representative liquefaction-induced building settlement and building interaction case histories are discussed and key insights are shared.

^{a)}Department of Civil and Environmental Engineering, Portland State University, 1930 SW 4th Ave, Portland OR 97201 b)Department of Civil and Environmental Engineering, University of California – Berkeley, 453 Davis Hall, Berkeley CA

Department of Civil and Environmental Engineering, University of California – Berkeley, 453 Davis Hall, Berkeley CA 94720

^{c)}Department of Civil, Environmental and Geodetic Engineering, The Ohio State University, 2036 Neil Ave, Columbus OH 43210

d)School of Civil and Environmental Engineering, Georgia Institute of Technology, 790 Atlantic Dr NW, Atlanta GA 30332 e)Southwest Research Institute, 6220 Culebra Rd., San Antonio, TX 78238

f)Department of Civil Engineering, Middle Eastern Technical University, Üniversiteler Mah. Dumlupınar Blv. No:1 06800 Ankara, TR

g)Zemin Etüd ve Tasarim A.Ş., Reşadiye Cad. No: 69/E 34794, Istanbul, TR

h)Department of Civil end Environmental Engineering, University of California Los Angeles, 580 Portola Plaza, Los Angeles CA 90095

i)Department of Civil Engineering, Iskenderun Technical University, 31200, İskenderun TR

INTRODUCTION

Significant and widespread liquefaction occurred in İskenderun due to the 2023 moment magnitude (M_w) 7.8 mainshock of the Kahramanmaraş earthquake sequence. Liquefaction and building damage were concentrated in the Çay District and in other areas of reclaimed land and near the historic shoreline. Liquefaction-induced building settlements from 0 to 740 mm were measured in İskenderun by the Geotechnical Extreme Events Reconnaissance (GEER) team. Building settlement affected the patterns of ground deformation observed adjacent to many structures. Often liquefaction-induced building settlement appeared to depress the ground surrounding the building downwards over several meters in a convex deformation pattern called hogging. Sagging was sometimes observed over wide buildings supported on shallow foundations. This paper summarizes observations of liquefaction-induced building and ground settlements in İskenderun, including liquefaction effects on building and interactions between nearby buildings. Before discussing these observations, the geologic setting of İskenderun and seismic demand from key events of the 2023 Kahramanmaraş earthquake sequence are discussed.

GEOLOGIC SETTING & SUBSURFACE CONDITIONS

The areas of Iskenderun that were significantly affected by liquefaction are composed of Quaternary alluvium from coastal and fluvial processes, and fill for reclaimed land (Brehme et al., 2011). Figure 1 provides an overview of the areas of İskenderun addressed in this paper, including the areas of reclaimed land (shown by the hatched pattern). Based on three geophysical surveys conducted in the İskenderun region by Ozdemir et al. (2019), the thickness of Quaternary alluvium is estimated to be approximately 35-40 m. Beneath this alluvium, rock formations, including claystone, sandstone, and limestone, are encountered. Soil descriptions and standard penetration test (SPT) blow counts (N) from three borings in İskenderun are illustrated in Figure 2; the boring locations are included in Figure 1a. The profiles suggest that very loose to loose silty sand with some gravel underlies İskenderun to depths of at least 30 m. The SPT blow counts, which are uncorrected for hammer energy because this information is not available, ranged from 2 to 12 in the sand and are consistent with the very loose to loose description of the soil. Given the borings are not located on reclaimed land, the soils in the profiles are likely Quaternary alluvium deposits. The water level in these three borings is between 1.5 and 3 m below the ground surface, suggesting a shallow water table in the areas where major liquefaction was observed.

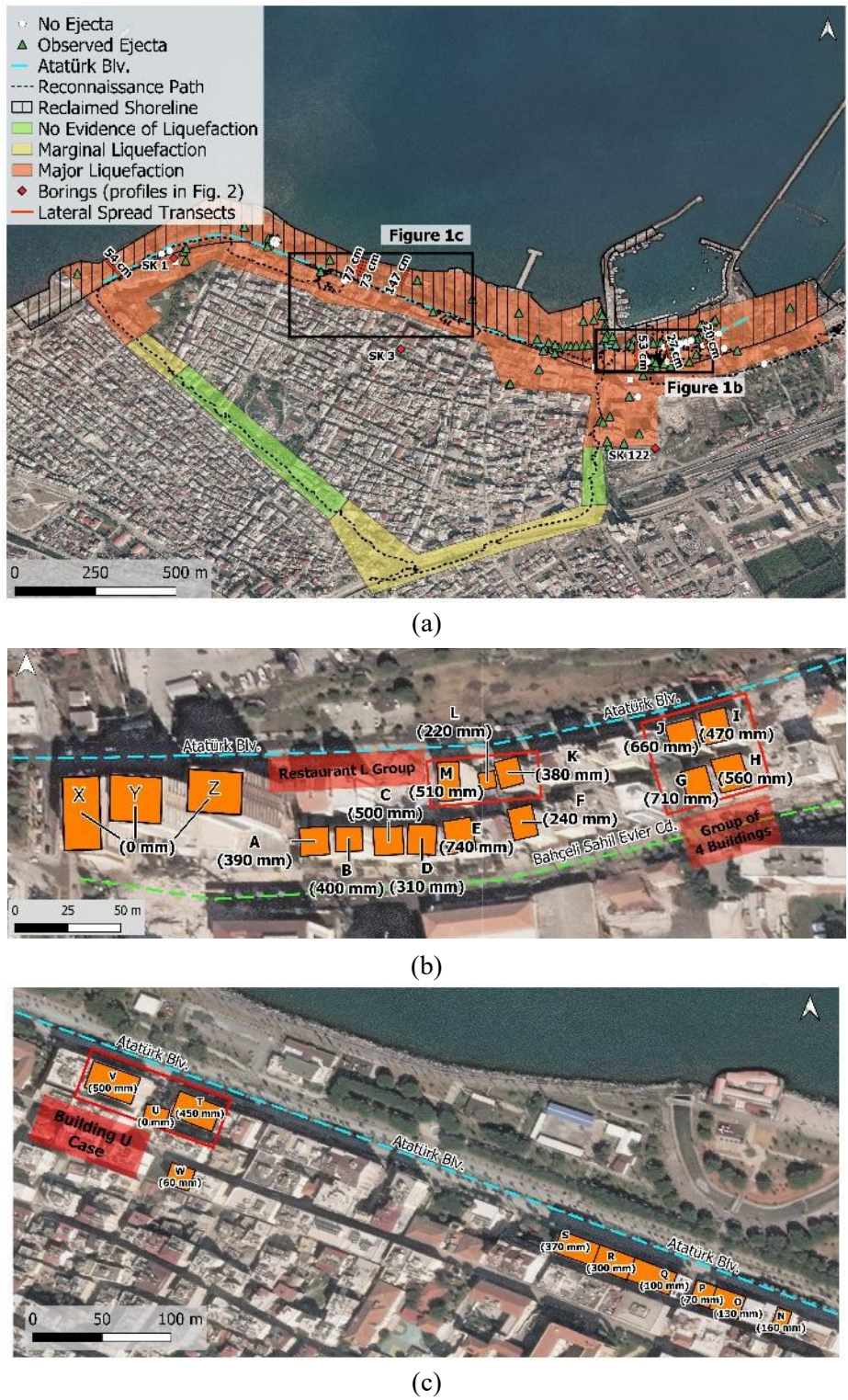


Figure 1. Overview of İskenderun reconnaissance: (a) İskenderun with interpreted areas of liquefaction, observed ejecta, reclaimed land, and lateral spreading. Areas of liquefaction are only inferred from areas where reconnaissance was performed, as shown by the shaded areas. (b) Buildings surveyed in the Çay District. (c) Buildings surveyed in the Yenişehir neighborhood. Each surveyed building is referenced by the letter shown, and the average building settlement is in parentheses. Base images were captured on February 12, 2023 from Maxar Technologies (2023).

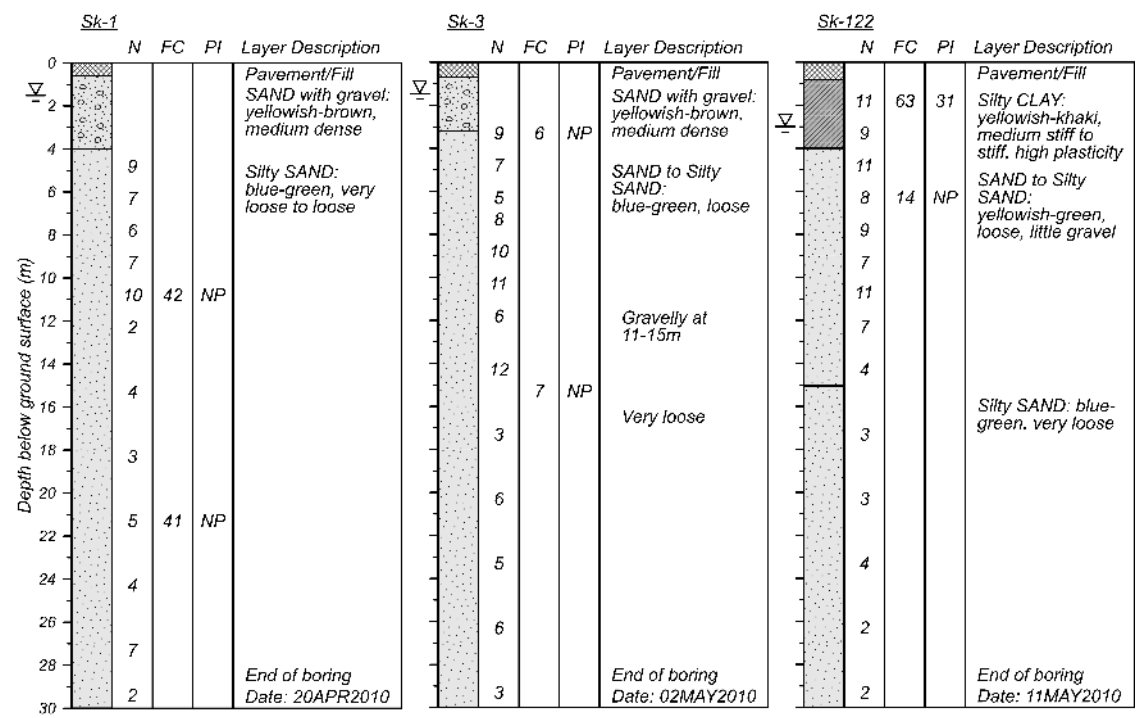


Figure 2. Representative subsurface conditions of northern İskenderun from borehole data from Orukoğlu & İşhani (2010). Boring locations are shown in Figure 1.

İskenderun is a historic port city that was developed primarily in the 20th century. The land around İskenderun is described in historical accounts as "swampy" and poorly drained; development of the city included large efforts to drain and fill the low-lying swampy areas (Nalça 2018). Development in the 20th century also included building out the shoreline with reclaimed land. The areas of reclaimed land in Figure 1a are interpreted from shorelines in historical maps dated before and in 1916; the historical maps are compiled in Nalça (2018). Atatürk Boulevard generally marks the boundary between the original land and reclaimed land. An example of the historic shoreline and current Atatürk Boulevard is shown in Figure 3. The same building (Building P in Figure 1c), formerly a community center and currently a civil registry, is pictured pre-1916 in Figure 3a and in May 2020 in Figure 3b. Pre-1916 the building was located along the shoreline; it is now located along Atatürk Boulevard and is 150 m from the current shoreline. Satellite imagery of İskenderun in 1969 presented in Taftsoglou et al. (2023) shows that some of the present-day reclaimed land was built out from Atatürk Boulevard at the time, including part of the Çay District. The historical maps and 1969 image suggest that the Çay District fill was placed between 1932 and 1969.



Figure 3. Example of historic development and reclaimed land in İskenderun. Building P, a former community center and current civil registry on Atatürk Boulevard, is shown in both images: (a) image that predates 1916 and along the former shoreline [date not known, obtained from Nalça (2018)], and (b) modern image of the building on Atatürk Boulevard [May 2020, obtained from Google Street View] (approximate coordinates 36.5916N 36.1702E).

İskenderun has been historically subjected to extensive damage and liquefaction from earthquake events, as documented in Ambraseys (1989). The August 13, 1822 earthquake, called the Aafrine or Aleppo earthquake, had an estimated M_w 7.5. Shaking from this earthquake event destroyed several houses and caused liquefaction along the coast. There are also accounts that groundwater levels rose above low lying ground for an extended period, turning cultivated land into marshy areas. These water level changes could be due to liquefaction subsidence or potentially tectonic subsidence. Strong shaking and damage in İskenderun is also reported from the April 3, 1872 M_w 7.2 Amik Gölü earthquake (Ambraseys, 1989).

SEISMIC DEMAND IN İSKENDERUN

The Kahramanmaraş earthquake sequence had two primary events: a $M_{\rm w}$ 7.8 mainshock that occurred on February 6, 2023 at 4:17 am local time, and a $M_{\rm w}$ 7.5 aftershock that occurred nine hours later. The Hatay region and İskenderun were also affected by a $M_{\rm w}$ 6.3 aftershock that occurred on February 20, 2023.

Ground motions near İskenderun were recorded by multiple strong motion stations (SMS). The locations of the 17 stations within 50 km of İskenderun are shown in Figure 4a; the locations within 25 km of the Çay District are shown by the red symbols. The closest stations to İskenderun are stations TK-3112, TK-3115, and TK-3116, which are labeled on Figure 4. Figure 4b shows the shear wave velocity (V_s) profiles for these stations, with average V_s values

over the top 30 m (V_{s30}) of 233 m/s, 424 m/s, and 870 m/s for the TK-3112, TK3115, and TK-3116 stations, respectively.

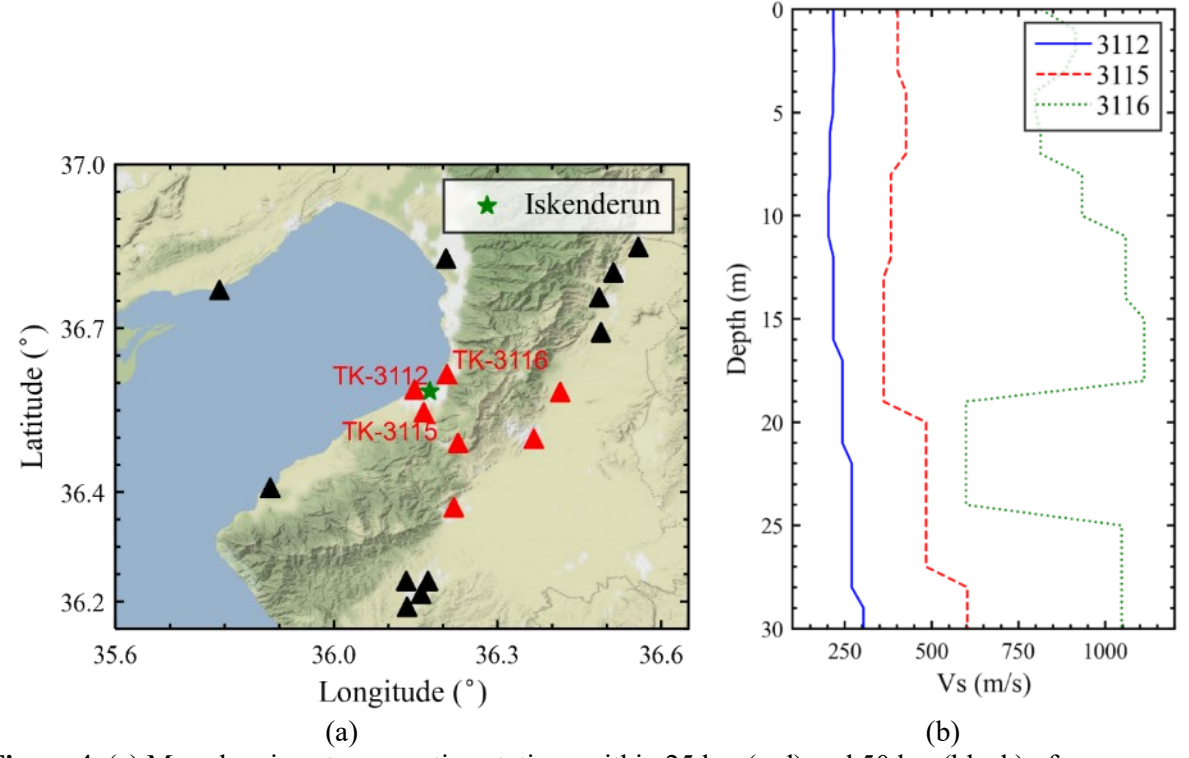


Figure 4. (a) Map showing strong motion stations within 25 km (red) and 50 km (black) of İskenderun; (b) shear wave velocity (V_s) profiles for stations TK-3112, TK-3115, and TK-3116 (source: METU EERC).

Figure 5 shows the 5%-damped acceleration response spectra of the East-West horizontal component of the recorded motions of the M_w 7.8 mainshock and M_w 6.3 aftershock at the TK-3112, TK-3115, and TK-3116 stations. The acceleration, velocity, and displacement time histories are also presented. TK-3112 had an early stoppage when recording the M_w 7.8 event; the stoppage appears to have occurred before the strongest shaking; hence, response spectra are not shown for this station. The V_s profile of station TK-3116 (V_s values higher than 800 m/s) suggests that the recorded motions can be considered as rock-like motions. There is a noticeable amplification of the acceleration response spectra of TK-3115 and TK-3112 when compared to that of TK-3116 for the M_w 6.3 aftershock, suggesting seismic site response effects in İskenderun and the Çay District.

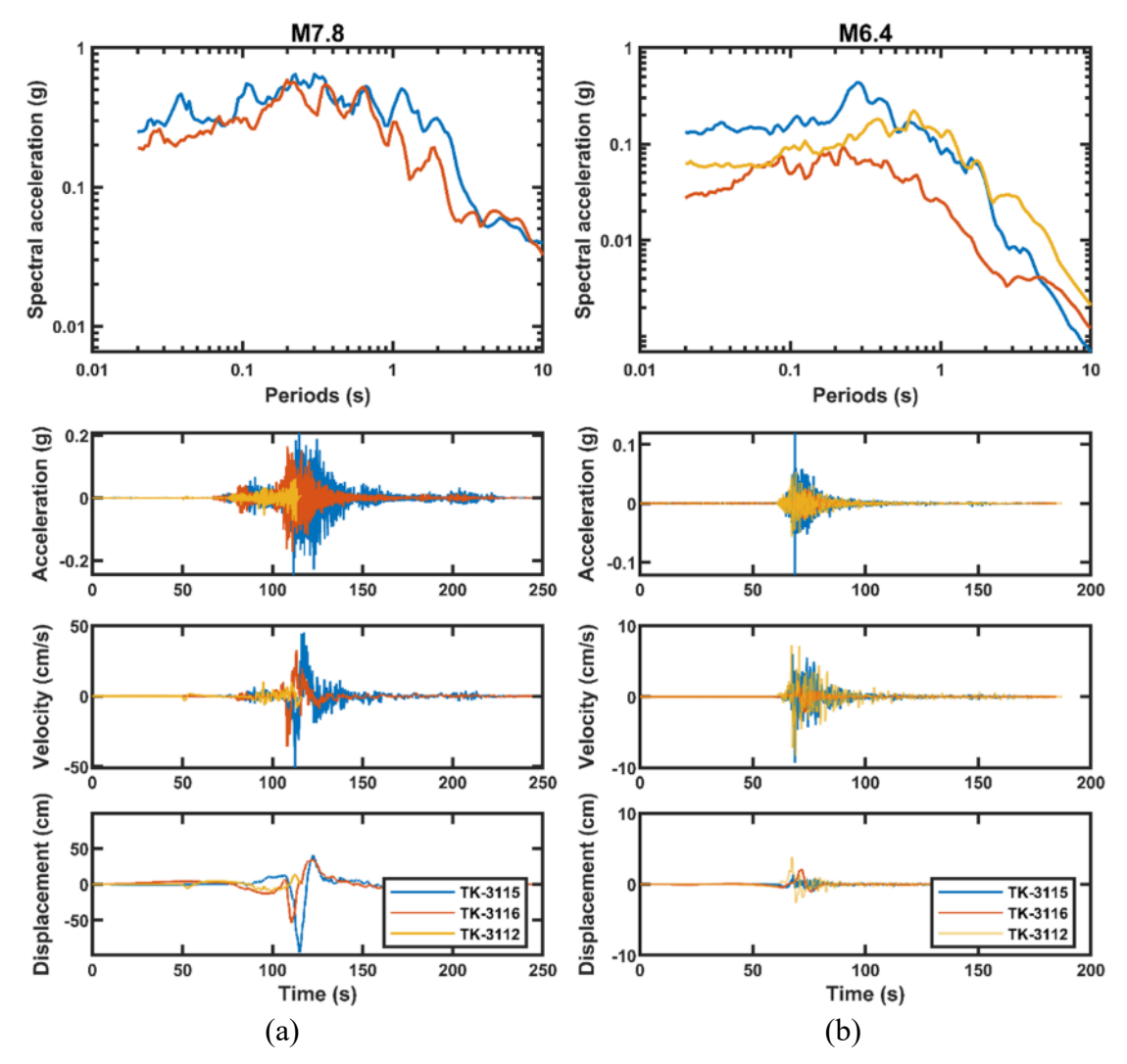


Figure 5. Ground motion time histories and 5%-damped acceleration response spectra for nearby seismic stations in Iskenderun. (a) M_w 7.8 mainshock was recorded fully at TK-3115 and TK-3116 and partially at TK-3112; (b) M_w 6.4 aftershock was recorded at TK-3112, TK-3115, and TK-3116.

Some intensity measures for the three events are summarized in Table 1; given the recording stoppage at TK-3112, intensity measures are not available from TK-3112 for the $M_{\rm w}$ 7.8 and $M_{\rm w}$ 7.7 events. However, the horizontal peak ground acceleration (PGA) in İskenderun can be estimated using the ground motion model presented in Buckreis et al. (2024, this collection) for the mainshock. The borehole profiles in Figure 2 indicate that there are loose silty sands to at least 30 m depth in areas of İskenderun, suggesting that the $V_{\rm s30}$ throughout north-central İskenderun is closest to that of TK-3112 (233 m/s) than the other strong motion stations. Assuming $V_{\rm s30}$ = 233 m/s and the event-corrected ground motion model (i.e., Kriging interpolation on within-event residuals), the horizontal PGA in the surveyed areas of İskenderun would be near 0.32 g, which is notably higher than the PGA values of 0.17g at TK-

3116 and 0.27 g at TK-3115 (values of intensity measures herein are the geometric mean of the north-south and east-west ground motion components). This level of amplification is consistent with the amplification observed in the M_w 6.3 aftershock. The cumulative absolute velocity (CAV) is known as an efficient intensity measure to assess liquefaction-induced damage (Bray and Macedo, 2017; Bullock et al., 2018). The recordings from the TK-3115 and TK-3116 stations show CAVs in the range of 1.5-3.0 g·s, which are significant. For context, the highest CAV during the Canterbury earthquake sequence was lower than 3.0 g·s (Bray and Macedo, 2017). With potential amplification effects, the CAVs in the liquefied areas of Iskenderun could be even higher than 3.0 g·s; however, ground motions in some areas may have been damped after liquefaction was triggered. The peak ground velocity (PGV) values from the M_w 7.8 are significant (and higher compared to the other events), suggesting potential near-fault region effects. The mean period (T_m) follows an expected trend, i.e., it increases as V_{s30} decreases; the estimated values also might be affected by potential near-fault effects. Recorded velocity pulses in the M_w 7.8 event suggest forward directivity effects in the region, which may have exacerbated the liquefaction consequences in Iskenderun. However, further investigation is needed into the near-fault and directivity effects at the İskenderun sites to understand the ground motion effects on these case histories.

Table 1. Intensity measures estimated from strong motion station recordings in the İskenderun area.

Table 1: Intensity incasures estimated from strong motion station recordings in the iskenderan are									
Intensity	M _w 7.8			M _w 7.7			M _w 6.3		
Measure	TK3116	TK3115	TK3112	TK3116	TK3115	TK3112	TK3116	TK3115	TK3112
Peak ground acceleration, PGA (g)	0.17 ^a / 0.17 ^b	0.25/ 0.29	-	0.02/ 0.02	0.03/ 0.03	-	0.03/ 0.04	0.12/ 0.11	0.06/ 0.09
Peak ground velocity, PGV (cm/s)	35.9/ 42.7	50.8/ 42.4	-	8.4/ 11.1	12.9/ 6.7	-	2.4/ 2.7	9.3/ 8.3	8.4/ 13.2
Mean period, T _m (s)	0.52/ 0.54	0.70/ 0.56	-	0.67/ 0.79	0.94/ 0.88	-	0.35/ 0.35	0.49/ 0.47	0.83/ 0.86
Cumulative absolute velocity, CAV (g·s)	1.46/ 1.47	2.39/ 3.00	-	0.20/ 0.18	0.35/ 0.37	-	0.14/ 0.16	0.42/ 0.44	0.37/ 0.35

^a east-west component, ^b north-south component

Ground motions and intensity measures within the areas of Iskenderun impacted by liquefaction will be studied further using site investigation data and site response analysis to estimate and refine seismic demand at the impacted sites while accounting for local site

conditions. However, these initial estimates and ground motion recordings provide context for the seismic demand that affected the areas investigated by the GEER team.

OVERVIEW OF LIQUEFACTION IN ISKENDERUN

Evidence of liquefaction, including large amounts of ejecta and lateral spreading, was observed in İskenderun following the 2023 Kahramanmaraş earthquake, as documented by Turkish-US GEER and Earthquake Engineering Research Institute (EERI) teams (e.g., Çetin et al. 2023, Moug et al. 2023). This evidence of liquefaction is attributed to the closer, larger magnitude of the February 6, 2023 M_w 7.8 mainshock within the Kahramanmaraş sequence. A detailed description of liquefaction manifestations, lateral spreading, and regional subsidence in İskenderun is presented in Bassal et al. (2024, this collection).

Figure 1a summarizes the evidence of liquefaction in the Çay District and north-central İskenderun observed by GEER teams in February and March 2023. Green triangle symbols in Figure 1a represent locations where liquefaction ejecta were observed by GEER teams, in photos uploaded to SiteEye (2023), or by residents. White circles represent locations where no liquefaction ejecta was observed. These locations of ejecta and no ejecta are provided as the locations captured by the photographs as opposed to the geotag of the camera location. The ejecta observations are limited to February 2023 since it was assumed that much of the ejecta was either degraded by flooding, rain, or wind or cleaned up before March 2023. Reconnaissance also confirmed that major liquefaction occurred at the İskenderun port (Çetin et al. 2023), located east of the area captured in Figure 1.

Lateral spreading was surveyed along the İskenderun shoreline through measured transects. The locations of these transects are included in Figure 1a. Details on the magnitude and extent of lateral spreading in İskenderun are provided by Bassal et al. (2024, this collection). The three transects in the Çay District revealed extensional ground cracks that extended from the shoreline to areas with buildings. It is possible that these ground cracks were indications of large-scale lateral spreading capable of influencing the observed building settlement. The building settlements reported in this study do not differentiate between different settlement mechanisms (e.g., shear, volumetric, ejecta, and lateral displacement), as there are insufficient data to be able to do so at this time. Follow-up studies may be able to collect sufficient data to understand better the contribution of different liquefaction-induced building settlement mechanisms (e.g., Bray and Macedo 2017).

Zones of "major liquefaction," "possible or marginal liquefaction," and "no evidence of liquefaction" are shown on Figure 1a. The zones are interpreted in areas where observations were made by GEER teams or SiteEye teams; this study does not provide an assessment of whether liquefaction did or did not occur outside of these zones. Representative GPS tracks of the GEER teams are shown in Figure 1a to provide the context of where the ground reconnaissance was performed in İskenderun. The zones of no evidence of liquefaction are areas where the teams deliberately looked for evidence of liquefaction (e.g., ejecta, settlement, rolled curbs), and none were observed. These zones include the southwestern part of Figure la, away from the shoreline. The zones of possible or marginal liquefaction are those where building settlement less than 30 mm was observed, and there was no surficial evidence of liquefaction. A possible or marginal liquefaction area is the underpass that runs approximately east-to-west through Iskenderun. Flooding and sand in the underpass were evident in aerial photos on Google Earth in the days following the earthquake, which was confirmed by a local taxicab driver. However, the only possible surface evidence of liquefaction was nearby buildings that appeared to have settled less than 30 mm. The flooding and sand may be evidence of subsurface buildup of excess porewater pressures that were relieved through the storm drains at the base of the underpass.

The zones of major liquefaction are associated with land between the historic shoreline and the current shoreline (i.e., reclaimed land) and near the historic shoreline. Liquefaction ejecta were observed south of the Çay District, about 200 m from the historic shoreline, and further from the historic shoreline than other observations of liquefaction in İskenderun. This occurrence could be associated with historic infill of low-lying swampy areas, historic depositional environment, or some other factor.

BUILDING-GROUND LIQUEFACTION INTERACTIONS

Overview of Building Settlement

Building settlements were predominately estimated through laser-level hand surveys and lidar scans at select buildings. The surveyed buildings in the paper are referred to by reference letters, as shown in Figures 1b and 1c, and by their location latitude and longitude. Laser-level hand surveys were performed by measuring settlement relative to a reference datum that was judged to have been minimally affected by earthquake shaking and liquefaction. An example of a laser-level hand survey at Building E (36.5902N 36.1777E) on Bahçeli Sahil Evler Street is shown in Figure 6a. Lidar scans used a terrestrial 3D scanner (FARO Focus3D X 330 2014)

to capture point clouds of the ground and buildings at 2 to 3 mm resolution. An example of a lidar scan being performed at Building K (36.5906N 36.1780E) on Atatürk Boulevard is shown in Figure 6b. Lidar scans at multiple locations around a building were registered together to create a three-dimensional (3D) model of a building and the surrounding ground. The lidar data were processed and registered in FARO Scene software (version 2023.0.1) and analyzed in the CloudCompare software (CloudCompare 2023). The analysis included estimating an original reference plane of the ground surface (i.e., the pre-earthquake ground surface) from ground points that were judged to be minimally affected by liquefaction and earthquake shaking and then calculating the vertical distance from the reference plane to the surveyed ground surface to create a ground settlement map. Building settlement was estimated from elevations at the bottom of the building (assumed to be in contact with the ground pre-earthquake) to the reference plane. A challenge of lidar analysis is shadowed zones where data points were not obtained. These data shadows primarily occurred near buildings where the ground was deformed downward by the building settling into foundation soils. In these cases of data shadows near buildings, the building settlements were estimated by referencing known heights or elevations of building features, including façade tile or balconies.

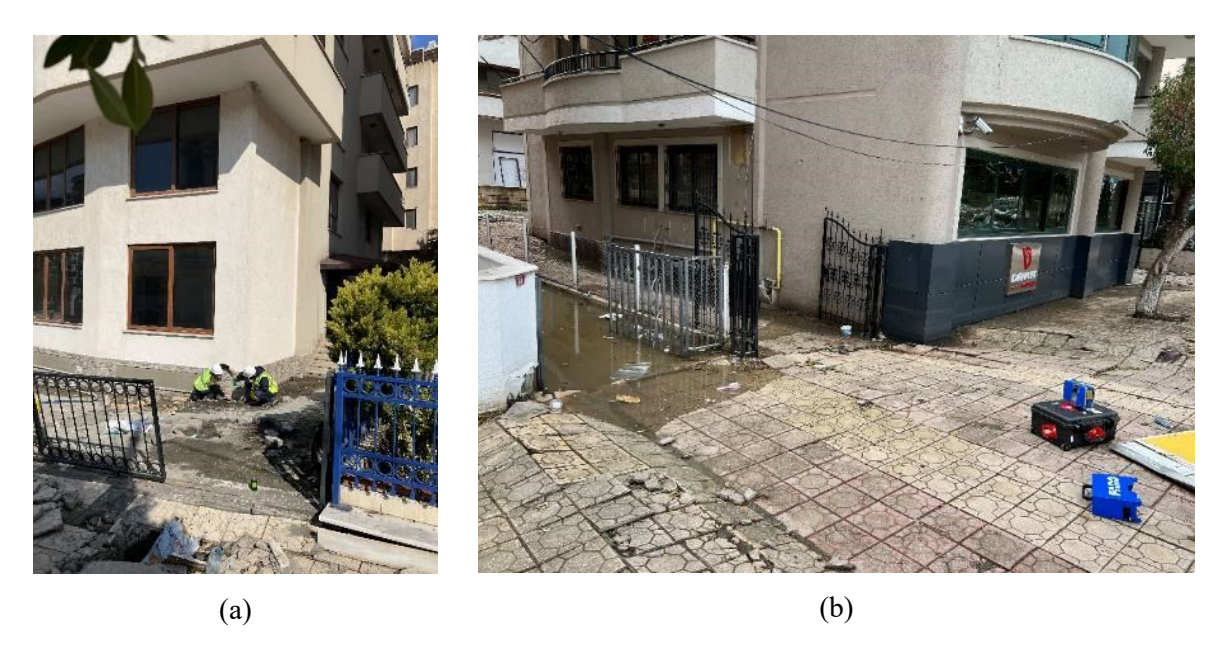
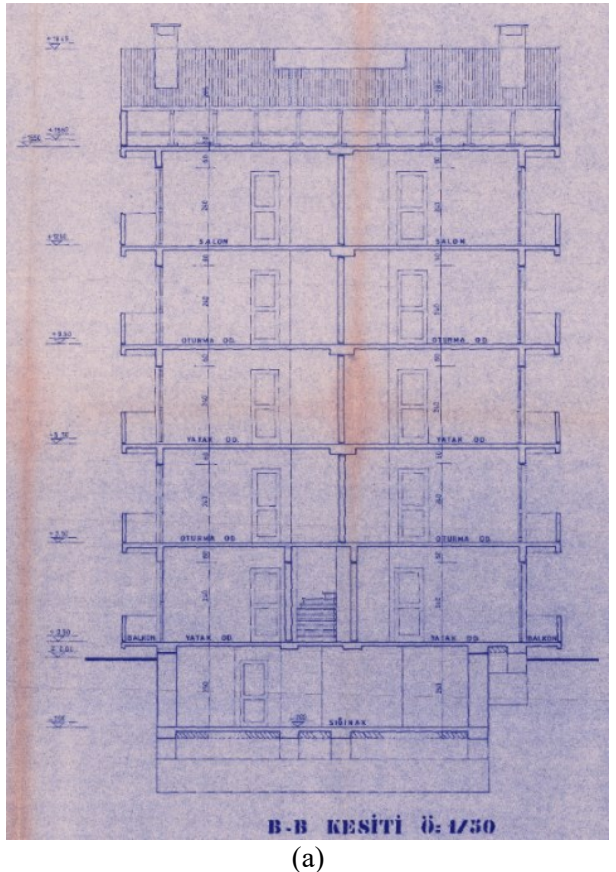


Figure 6. Examples of building settlement survey methods: (a) hand survey at Building E on Bahçeli Sahil Evler Street with a laser level where the laser level is placed on a reference ground level that was judged to have not settled (36.5901N 36.1778E; 28 MAR 2023), and (b) lidar scans at Building K on Atatürk Boulevard (36.5907N 36.1781E; 29 MAR 2023).

Buildings surveyed in the Çay District had settlements ranging from 0 mm to 740 mm. The significant amount of ejecta observed in the Çay District indicates these are liquefaction-induced building settlements. Figure 1b shows the surveyed buildings and their average settlement. They were largely reinforced concrete frame with infill walls (RCF-IW) structures. Sixteen buildings were surveyed in the Çay District. Twelve of the buildings were five- or six-story ("mid-rise") buildings with courtyards and side yards between each building, three were high-rise structures over eight stories high, and one had a single story. Settlements at the five and six-story buildings ranged from 240 mm to 740 mm, with all but one settling over 300 mm. The three high-rise buildings (Buildings X, Y and Z; 36.5904N 36.1762E), which were located adjacent to one another, had no discernable settlement (i.e., 0 mm of settlement). These buildings are assumed to be on pile foundations, given the height of the buildings founded on reclaimed land and their good foundation performance during the earthquake. The single-story building (Building L; 36.4806N 36.1778E) appeared to settle differentially due to influences from nearby buildings, with an average settlement of 220 mm; this building is presented with additional details below.

Building plans from two five-story buildings in the Çay District are shown Figure 7. These two building plans represent typical foundation types for mid-rise buildings in the Çay District. Figure 7a shows plans from Building D (36.5902N 36.1776E), which settled an average of 310 mm. Building D has a half basement across the front (south) half of the building; the cross section in Figure 7a pictures the half of the building with the basement. A mat foundation extends across the entire building footprint at 3.4 m depth; fill soil is in place above the mat in the non-basement area. Figure 7b is a plan view of the foundation of Building C (36.5902N 36.1774E). The foundation of Building C uses strip footings in orthogonal directions across the building footprint. Building C was surveyed with laser-level hand measurements and lidar scans; the settlement at Building C is estimated to be 500 mm on average.



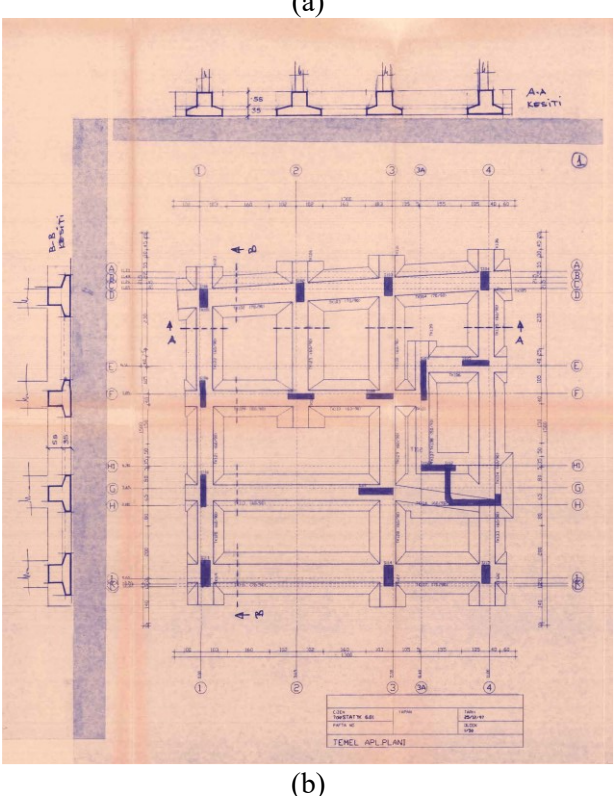


Figure 7. Building plans for two buildings in the Cay District: (a) cross-section view of Building D (36.5902N 36.1776E) on Bahçeli Sahil Evler Street showing the mat foundation; (b) plan view of foundation at Building C (36.5902N 36.1774E) on Bahçeli Sahil Evler Street showing the strip footings that orthogonally intersect.

Nine buildings were surveyed in the Yenişehir neighborhood, with average settlements ranging from 0 mm to 520 mm (Figure 1c). The largest building settlements were measured near the historic shoreline and then decreased with distance inland from the historic shoreline. For instance, settlements up to 520 mm were measured at buildings surveyed along Atatürk Boulevard. Settlements less than 100 mm were apparent at Building P (36.5916N 36.1702E, pictured in Figure 3), which had an average 70 mm of settlement, and Building W (36.5925N 36.1660E) on Mareşal Fevzi Çakmak Street, one block south of Atatürk Boulevard, which had an average settlement of 60 mm (discussed below). As noted above, the areas of minor or marginal liquefaction in Figure 1a include those where < 30 mm of building settlement were observed, further supporting that liquefaction-induced building settlements decreased inland from the historic shoreline.

Settlement was observed across a block of adjacent buildings along Atatürk Boulevard in the Yenişehir neighborhood (shown in Figure 8), providing an example of settlement for closely spaced buildings along the historic shoreline. The eastmost building is Building Q (36.5917N 36.1699E). Negligible settlement was observed at the east corner of Building Q (32.45 m wide) and 210 mm at its west corner. The middle building, Building R (36.5918N 36.1696E; 25.33 m wide), settled 210 mm at its east corner and 380 mm at its west corner. The westernmost building, Building S (36.5919N 36.1693E; 40.55 m wide), settled 410 mm at its east corner and 320 mm at its west corner. The presence of standing water in Figure 8b follows the pattern of observed settlement; standing water is present at Buildings R and S where larger settlements were measured compared to Building Q.



Figure 8. (a) Photo of adjacent buildings Q, R, and S with settlement measurements (36.5924N 36.1690E; 1 APR 2023), (b) same group of buildings with Building Q in the foreground and including standing flood water on front sidewalk in front of buildings R and S (36.5916N 36.1700E; 1 APR 2023).

Detailed Examples of Liquefaction-Induced Building Settlement

Building B on Bahçeli Sahil Evler Street (36.5902N 36.1772E) was surveyed with laser level hand survey, lidar scans, and photogrammetry that was subsequently combined with lidar data. The street view of the building is shown in Figure 9a. Building B is a six-story residential RCF-IW structure. There was no apparent basement, however, there was a sub-ground level room for the electrical panel. A summary of the building settlement estimates by hand survey and lidar scan data is provided in Figure 9b. The average building settlement by lidar scan analysis is 400 mm. There are discrepancies between the hand survey and lidar analysis estimates of settlement at the west side of this building. This likely reflects difficulties in finding a reliable datum (i.e., a point at which the ground elevation was not affected by earthquake deformations) and referencing each corner of the building to this point. The lidar scan estimates are considered more reliable than the hand survey estimates because of the detail captured by lidar scans and the ability to re-analyze the point cloud.

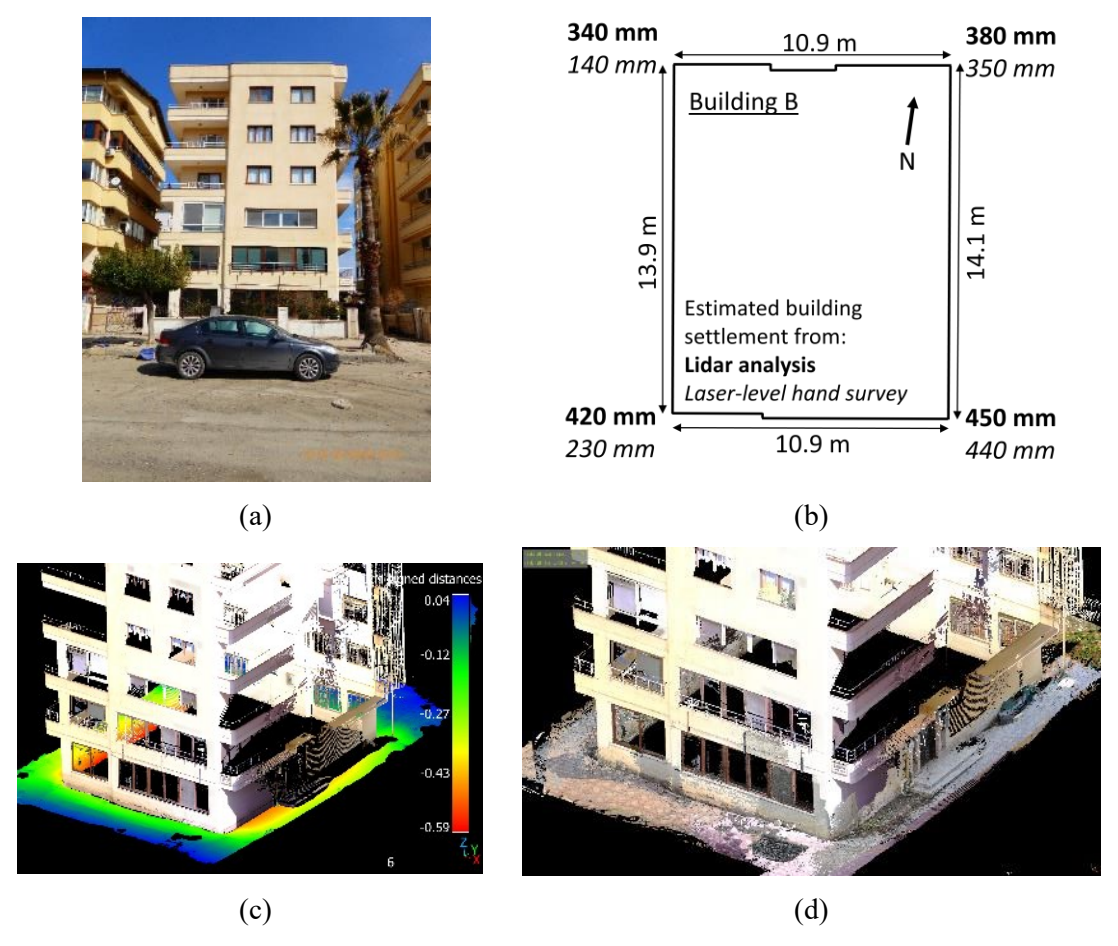


Figure 9. Building B on Bahçeli Sahil Evler Street in the Çay District: (a) street view of the building (36.5900N 36.1772E; 28 MAR 2023); (b) summary of survey measurements from various methods; (c) lidar scan of the building with contours of ground settlement (in m); (d) combined photogrammetry and lidar data also showing ground deformation around the structure.

Lidar scans were performed at the four corners of Building B. A reference ground plane that slopes 1° from north (rear of the property) to south (front of the property) was fit to the ground elevation data; this plane represents the assumed pre-earthquake ground elevation. The ground contours in Figure 9c represent the difference between the scanned ground elevation and the reference plane (i.e., contours of ground settlement due to the earthquake event). The ground deformation shows settlement around the building extends over 2 m around the building footprint. As evident in Figure 9c, there were data shadows in the lidar scans, particularly around the base of the building. At the building's northeast corner, the ground adjacent to the building was largely shadowed, not allowing the ground elevation to be analyzed in this area. Combining the lidar data with photogrammetry can fill in these data shadows. Photogrammetry was performed by stitching many high-resolution photos obtained from the scanner into a 3D model. The result of combining the lidar and 3D photogrammetry is shown in Figure 9d, showing that photogrammetry was able to compensate for several of the areas shadowed in the lidar data, including the ground near the east side of the building.

Building E on Bahçeli Sahil Evler Street (36.5902N 36.1777E) provided an example of the influence of the building foundation type on building-ground interactions. Building E is a five-story residential RCF-IW structure; the building's street view is shown in Figure 10a. The building owner reported that the structure has a 2.8 m deep basement with a 40 cm thick reinforced concrete mat foundation that extends out 1.5 m around the footprint of the building. The average building settlement was estimated to be 740 mm from combined laser-level hand surveys and lidar scan data. Figure 10b shows the effect of the building foundation on ground deformations, where a depression that coincided with the foundation mat was observed around the building. The settlement at this building was the largest of the buildings surveyed in the Çay District. The foundation type appeared to be unique among the buildings surveyed in the Cay District: few buildings had full basements without pile foundations, and there were no other similar ground deformation patterns that could be attributed to a foundation mat that extended a similar distance around the building footprint. The large liquefaction-induced settlements at Building E likely indicate poor ground conditions.

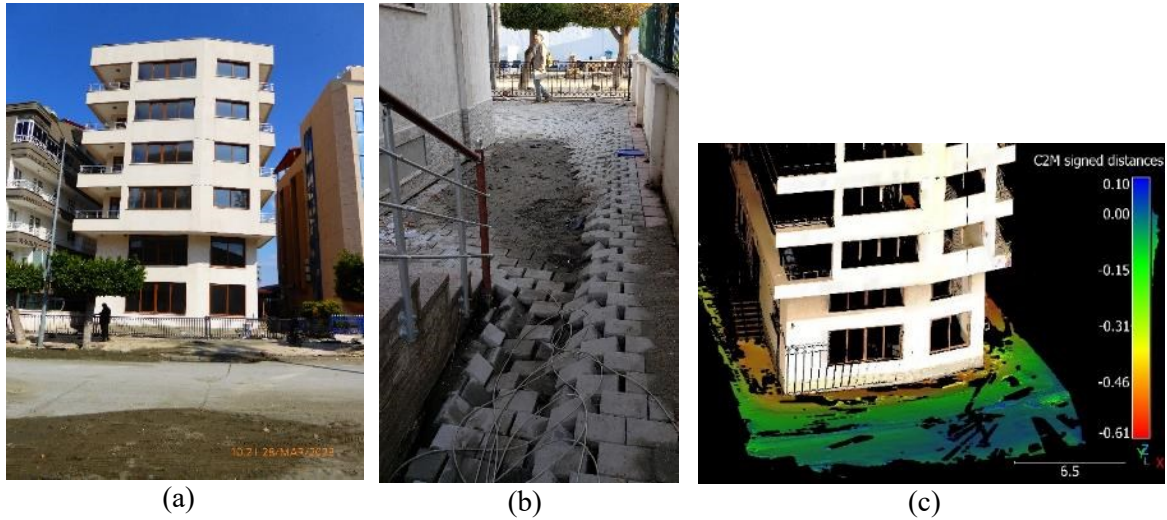


Figure 10. Building E on Bahçeli Sahil Evler Street in the Çay District: (a) street view of the building (36.5899N 36.1779E; 28 MAR 2023), (b) west side of the building showing the effect of the building foundation on ground deformation and settlement (36.5903N 36.1776E; 27 MAR 2023), and (c) lidar scan of ground settlement (in m) and the building.

Buildings on pile foundations generally performed well, with little liquefaction-induced settlement observed. In addition to the three high-rise buildings with no noticeable settlement described in the previous section, Building F on Bahçeli Sahil Evler Street (36.5903N 36.1781E; shown in Figure 11a) settled less than the other buildings without deep foundations surveyed in the Çay District. The building owner reported that the foundation has a full basement with concrete piles. A settlement of 240 mm was estimated at Building F from a laser-level hand survey and from a lidar scan at the northwest corner. Building settlement also deformed the ground around the building; Figure 11b shows the rear courtyard (north side of the building), where there is an apparent slope in the ground from the partition wall towards the building. The ground pavers around the partition wall in Figure 11b show additional ground settlement, which may be attributed to poor fill compaction close to the wall, ground extension from nearby lateral spreading, ground extension from building settlement-induced ground deformations, or some combination of these factors. The contoured lidar ground data at the rear courtyard in Figure 11c further show these building settlement-induced ground deformations, where lidar data indicate ground settlement extends over 2 m from the building. The ground to the west of Building F and on the right of Figure 11c had a depression that did not appear to be related to liquefaction settlement, and was likely due to erosion during flooding or poor fill compaction around the basement.



Figure 11. Building F on Bahçeli Sahil Evler Street in the Çay District: (a) street view of the building (36.5900N 36.1782E; 28 MAR 2023), (b) north side of the building showing the ground deformation and settlement (36.5903N 36.1780E; 28 MAR 2023), and (c) lidar scan data showing ground deformation patterns around the structure.

BUILDING-GROUND INTERACTIONS

Hogging Building-Ground Interactions

Documented building-ground interactions in the Cay District and Iskenderun indicate a distinct pattern of ground deformations induced by building settlement. It appeared that building settlement dragged down adjacent ground over a length of several meters from the building edges, with the ground settlement decreasing with increasing distance from the building. This resulted in convex ground surfaces near the buildings as depicted in Figure 12 and described herein as a "hogging" pattern of ground deformation. The hogging ground deformation was observed in the ground surrounding buildings that settled significantly, which differs from hogging due to differential building settlement with the exterior of a foundation settling more than the center. Most of the buildings in the Cay District and Iskenderun had stiff foundations that appeared to settle without significant internal distortion. Free-field observations did not provide evidence of ground settlement or heave that would be an alternate explanation for the observed hogging ground deformation surrounding buildings that settled significantly. In addition to the building settlement associated with ground hogging, some punching settlement was observed where the building settled into the ground immediately adjacent to the building. However, in general, the punching settlement was notably less than the building settlement associated with ground hogging settlement throughout the Cay District and İskenderun.

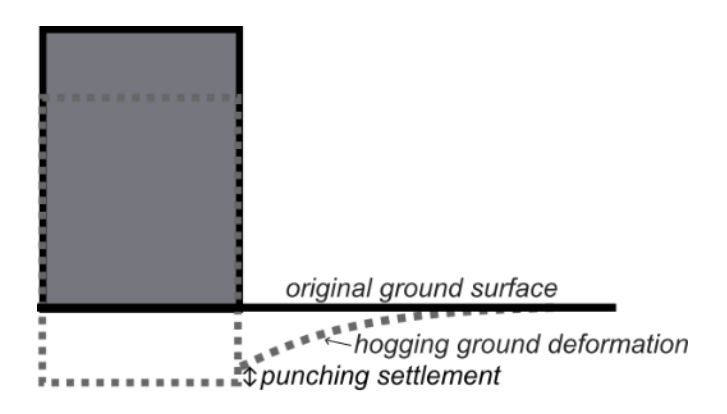


Figure 12. A schematic of building-ground interaction observed at several sites in İskenderun with contributions from punching and building-induced ground hogging. The dashed line represents the post-earthquake building and ground; the solid line represents the original ground surface and building.

Three representative cases of hogging building-ground interaction were documented in detail. These three cases are for hogging deformation between two buildings and are distinguished by the spacing between buildings and how nearby buildings were affected by the building-induced ground deformation. The observed cases had access between the buildings, and the buildings were spaced far enough apart to allow unobstructed observations of the building-ground interactions. It is likely that similar ground deformations and building-ground interactions occurred throughout liquefied areas in İskenderun, including for the building cases previously described; however, building spacing, building collapse, features like fences and landscaping, and available time did not allow observations of similar building-ground interactions between two buildings.

Building U, Yenişehir neighborhood

Hogging ground deformation was observed at Building U (36.5930N 36.1657E) on Atatürk Boulevard in the Yenişehir district. The hogging ground deformation developed between two six-story RCF-IW structures: Building T (36.5930N 36.1661E; east of Building U in Figure 13a) and Building V (36.5932N 36.1655E; west of Building U in Figure 13c). Building U sits between these buildings in the background of Figure 13b. Building T settled an average of 450 mm, and Building V settled an average of 500 mm; at the building corners along Atatürk Boulevard and closest to Building U, Building T settled 420 mm, and Building V settled 450 mm. There was no discernible building settlement at Building U. All settlements at this site were performed with hand laser-level measurements. Building U was built before 1946, although the construction date is not known at this time. Building T was measured to be 16.8 m in width (i.e., parallel to Atatürk Boulevard), estimated to be 22.5 m in length (i.e., orthogonal to Atatürk Boulevard) by Google Earth, and 18.7 m in height. Building V was measured to be

36.4 m in width, estimated to be 25.3 m in length by Google Earth, and 21.8 m in height. The total distance between Buildings T and V is 28.8 m. The manager of Building U reported that Building T does not have a basement, and it is also likely Building V does not have a basement.



Figure 13. Buildings T, U, and V on Atatürk Boulevard in İskenderun. (a) Building to the east of Building U (Building T) where liquefaction-induced settlement caused hogging deformation to the nearby ground (36.5928N 36.1661E; 28 MAR 2023), (b) Building U, which appeared unaffected by liquefaction (36.5935N 36.1660E; 16 FEB 2023). (c) Building to the west of Building U (Building V) where liquefaction-induced settlement also caused hogging deformation to the nearby ground (36.5928N 36.1661E; 28 MAR 2023). The photo in Figure 12b is credited to Eylem Arslan and retrieved from SiteEye.

The settlement of Buildings T and V appeared to drag down the surrounding ground in the same pattern as shown in Figure 12. There was a diminishing amount of depressed ground surface extending out from the buildings until it was no longer noticeable. Because there were contributions from both buildings on either side of Building U, the hogging ground deformation pattern in Figure 12 is horizontally mirrored. The central horizontal segment between the convex ground deformations, and where there was no apparent ground settlement, was about 9 m long. This central area appears to be free-field conditions, which is also supported by observations of negligible settlement and damage at Building U. Therefore, the zone of influence over which the hogging deformations extended is about 9.9 m from both Buildings T and V. Given the observations of widespread liquefaction, it is likely that the entire area also settled. However, this interpretation assumes that the area around these buildings is equally affected by this widespread settlement, which does not significantly affect these localized building-ground interactions.

Group of four buildings, Çay District

Hogging ground deformation was also observed in the courtyard between two sets of two similar buildings in the Çay District. Figure 14 shows the courtyard between the buildings with the hogging ground settlement pattern between the buildings; the convex warped ground is also apparent through the spreading of the ground tiles and floodwater present only around the base of the buildings (photographs were taken on March 29, 2023 when there was significant flooding in the Çay District and İskenderun).



Figure 14. Building-ground interactions between four buildings in the Cay district resulting in hogging ground deformation (a) facing west with Building G on the left and Building J on the right; (b) facing east with Building I on the left and Building H on the right. Both photos were taken from the same location (36.5906N 36.1790E; 29 MAR 2023).

The plan view of the set of four buildings, including dimensions and estimated settlements, is shown in Figure 15. The two west structures, Building J (36.5907N 36.4789E) located on Atatürk Boulevard, and Building G (36.5905N 36.1790E) located on Bahçeli Sahil Evler Street, appear to have similar design, age, and construction. These two structures were built prior to September 2007, according to Google Earth imagery. Similarly, the two east structures, Building I (36.5908N 36.1791E) located on Atatürk Boulevard, and Building H (36.5906N 36.1792E) located on Bahçeli Sahil Evler Street, also appear to have similar design, age, and construction. These two structures were built between September 2007 and 2010 based on Google Earth images. All the structures appear to be RCF-IW structures, six stories high with a half-seventh story. There were no apparent basements for the buildings; however, there were sub-ground level utility rooms on the east side of Buildings I and H and on the west side of Buildings J and G.

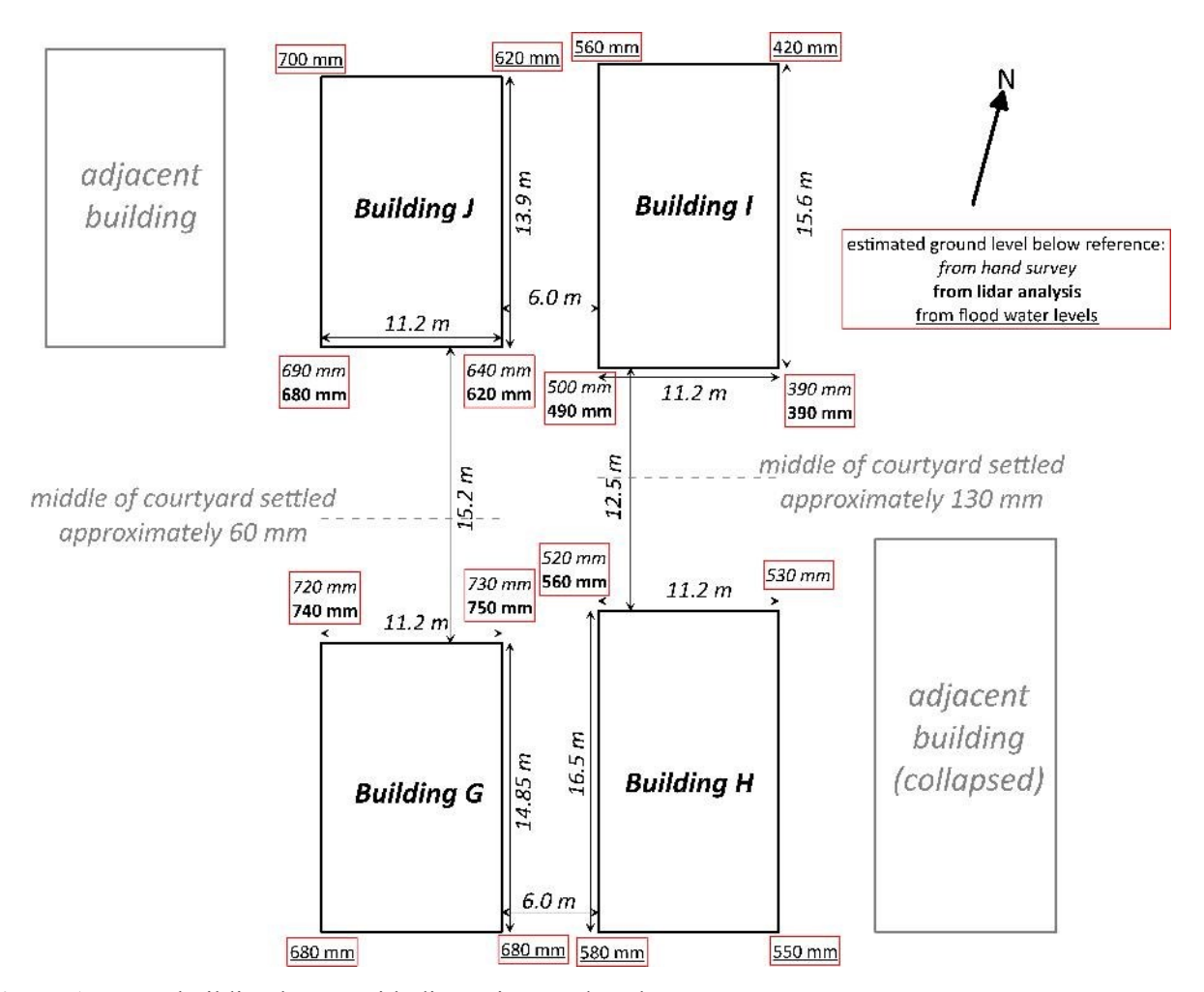


Figure 15. Four-building layout with dimensions and settlement measurements.

Settlement at the corners of the buildings was estimated from a combination of hand laser-level measurements, lidar scan data, and flood water depth during the March 29, 2023 flood event. The flood water was used to estimate settlements by measuring flood water depth from the building base and then referencing that depth to a location where settlement could be measured by hand survey or lidar. The flood water approach assumed consistent water surface elevation during measurements and was only used at locations that could not be surveyed otherwise. Settlement estimates were generally consistent between lidar and laser-level approaches, with differences being less than 40 mm or 10%. Average settlements were significant at all buildings, with 560 mm, 710 mm, 660 mm, and 470 mm estimated for Buildings H, G, J, and I, respectively. The settlements of Buildings H and I were similar, as were the settlements of Buildings G and J; however, the settlements of the pairs of buildings differed. It is unknown if the difference in the pair of building settlements is due to differing

ground conditions, different design and construction details, or influence from adjacent buildings (discussed further below).

Lidar scans performed on March 29 and April 1, 2023 captured ground settlement between the four buildings, which displayed a hogging ground deformation pattern from all four buildings. Figure 16 provides contours of vertical distance from a horizontal reference plane. The original ground elevation is estimated from the elevations at the sides of the courtyard, not directly between the buildings because the lidar data show the sides of the courtyard are at a higher elevation than the areas between the buildings. The settlement contours indicate the least ground settlement occurred in the middle of the courtyard between the buildings, and ground settlement increased towards the buildings. Six profiles of ground surface deformation in the courtyard between the four buildings were extracted from the lidar data and plotted in Figure 17; the locations of these profiles are shown by the red lines in Figure 16a. The ground settlement of these six profiles between the buildings is relative to the interpreted initial ground elevation. The ground deformations show distinct warping of the ground from individual buildings, consistent with the interpreted pattern in Figure 12. The average building settlements measured on the courtyard side of the buildings are plotted as the triangle symbols for Buildings H and I and the circle symbols for Buildings G and J in Figure 17. As plotted in Figure 17, the building settlement measurements fall into a similar pattern as the ground deformation between the buildings, with some variation due to measurement variability and other potential settlement mechanisms (e.g., punching shear failure, global seaward lateral spreading); however, the supporting evidence suggests the ground deformation patterns of the ground adjacent to the buildings relate strongly to building settlements.

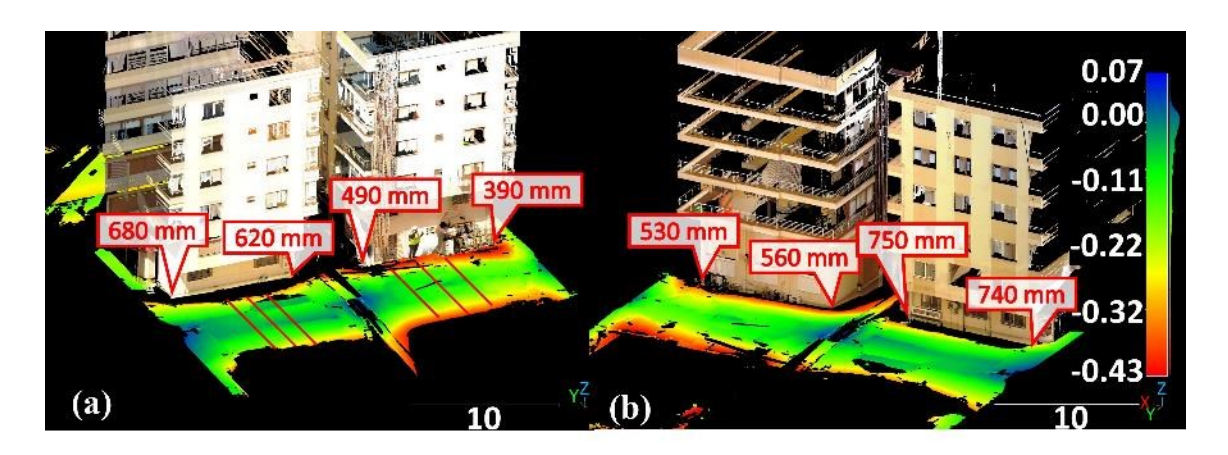


Figure 16. Four-building group: (a) lidar scan data facing the north buildings with Building J on the left and Building I on the right. The red lines represent locations of ground deformation profiles in Figure 17; (b) lidar scan data facing south buildings with Building H on the left and Building G on the right. Called out numbers are the building settlements from lidar or hand survey (if lidar not available). Color scale represents the ground distance from the initial reference plan (in m). Note that data shadows prevent lidar data from extending to the base of the buildings in most cases.

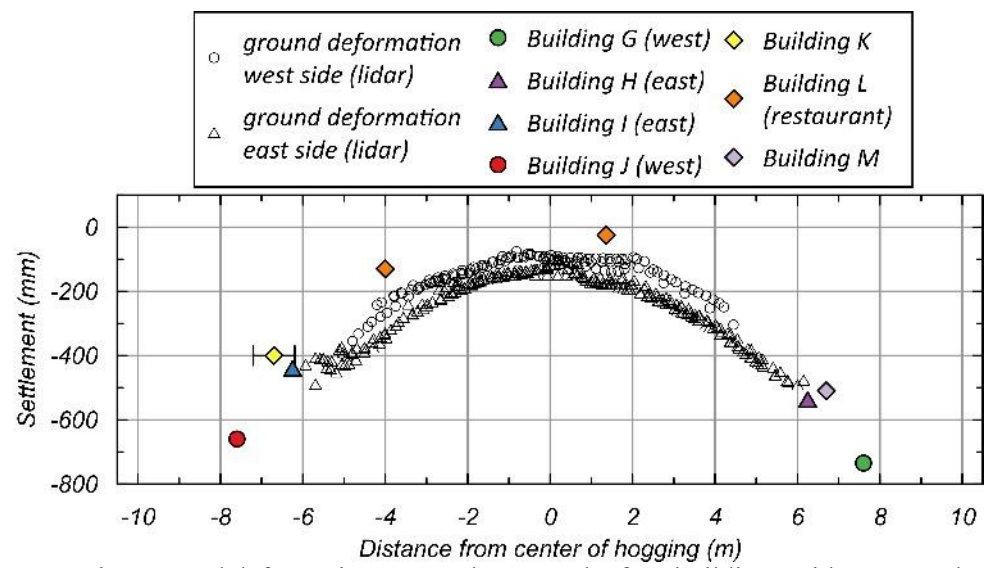


Figure 17. Hogging ground deformation pattern between the four buildings with measured settlements at other sites where hogging ground deformation was observed. Settlement of the K, L, and M buildings are also shown.

Elevation differences between the middle of the courtyard and the reference planes indicate that free-field conditions did not exist between the buildings, and there were likely interactions between the ground deformations induced by the settlements of each building. The area between Buildings G and J is 60 mm lower than at the west edge of the courtyard (where it is assumed that the ground did not settle), and the area between the Buildings H and I is 130 mm lower than at the east edge of the courtyard (where it is also assumed that the ground did not settle). A schematic of the interpreted building-ground interaction between these buildings is illustrated in Figure 18, including the overlapping of the zones of influence between the

buildings. There were likely similar interactions between adjacent buildings (e.g., between Buildings J and I and between Buildings H and G) where there is about 6 m separation between buildings. For instance, Figure 19 shows ground deformations and bending to the west of Building G, where there is an empty lot to its west.

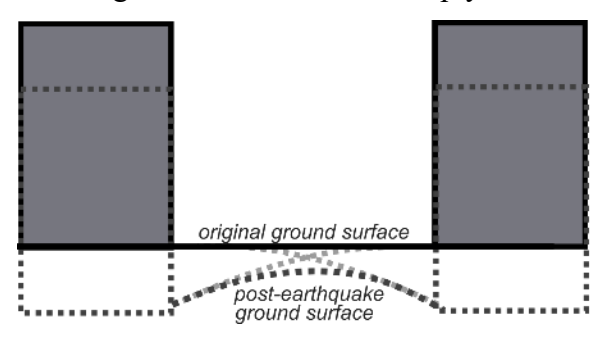


Figure 18. A schematic of interpreted building-ground interactions at the group of 4 buildings. The post-earthquake building settlement and ground is shown by the dark dashed lines, which is the result of overlapping ground deformation from each building (light grey dashed lines); the original ground surface is the solid black line.



Figure 19. Ground deformation to the west of Building G (36.5904N 36.1790E; 15 FEB 2023).

The influence of settlement at adjacent buildings can possibly explain observed differential ground settlements or varying performance between similar buildings. Although the buildings to the east and west of the group of four buildings were not surveyed, some discussion of their influence is merited. There was an empty lot to the east of Building I; the settlement measured on the east side of Building I is 100 mm to 140 mm less than the west side, where the settlement of Building J may have dragged down the west side and the east side was not affected by an adjacent building. There was a building to the east of Building H that collapsed after the earthquake event. Settlement of Building H is relatively uniform from the east to west sides of

the building, possibly attributable to buildings to both the east and west influencing ground deformations in addition to settlement at Building H itself. However, there was no building to the west of Building G, and there are no distinct differential settlements at Building G. This is possibly due to large settlements from Building G relative to Building H obscuring influence from the adjacent building. There is a building to the west of Building J and settlements on the west side of Building J were 50 to 80 mm larger than on the east side. If settlement at the adjacent building was significantly larger than at Building J, this may account for the differential settlements. These observations indicate that adjacent building settlements possibly affected settlement at some buildings; however, further investigation is warranted to examine this issue comprehensively.

Building L Restaurant, Çay District

A three-building group of Building K (36.5906N 36.1780E), Building L (36.5905N 36.1778E; a restaurant), and Building M (36.5905N 36.1777E) on Atatürk Boulevard in the Çay District provides an example of the effect of the hogging ground deformation on buildings. The three buildings are shown in Figure 20a. Large settlement of two tall RCF-IW structures (Buildings K and M) appeared to induce the hogging ground deformation beneath the middle lightweight single-story steel-frame structure of Building L. Building M has six full floors with a half-seventh floor (rubble around Building M limited access to the structure) and Building K has five full floors and a partial sublevel associated with the elevator. An in-depth survey of Building K was performed, and details are provided in Moug et al. (2023). The Building L restaurant is 10.7 m wide along Atatürk Blvd. Building M is directly adjacent to the restaurant building, whereas Building K is approximately 2.7 m from the restaurant based on estimates from pictures and Google Earth.

The hogging ground deformation induced by the settlement of Buildings K and M distorted the restaurant structure. Settlement was surveyed at Building L in reference to a point on the sidewalk in front of the building. These settlements, summarized in Figure 20a, measured 200 mm at the center of the structure, 130 mm at the east corner of the front retaining wall and 510 mm at the west corner of the front retaining wall. To the west of Building L, Building M settled 510 mm at its front. To the east of Building L, Building K settled 400 mm at its corner closest to Building L. Damage at Building L is highlighted in Figure 20b and included extension cracks in the façade and to the concrete floor slab, which are consistent with the observed hogging ground deformation pattern. Measurements of cracking in the interior floor were not taken as it was unsafe to do so.

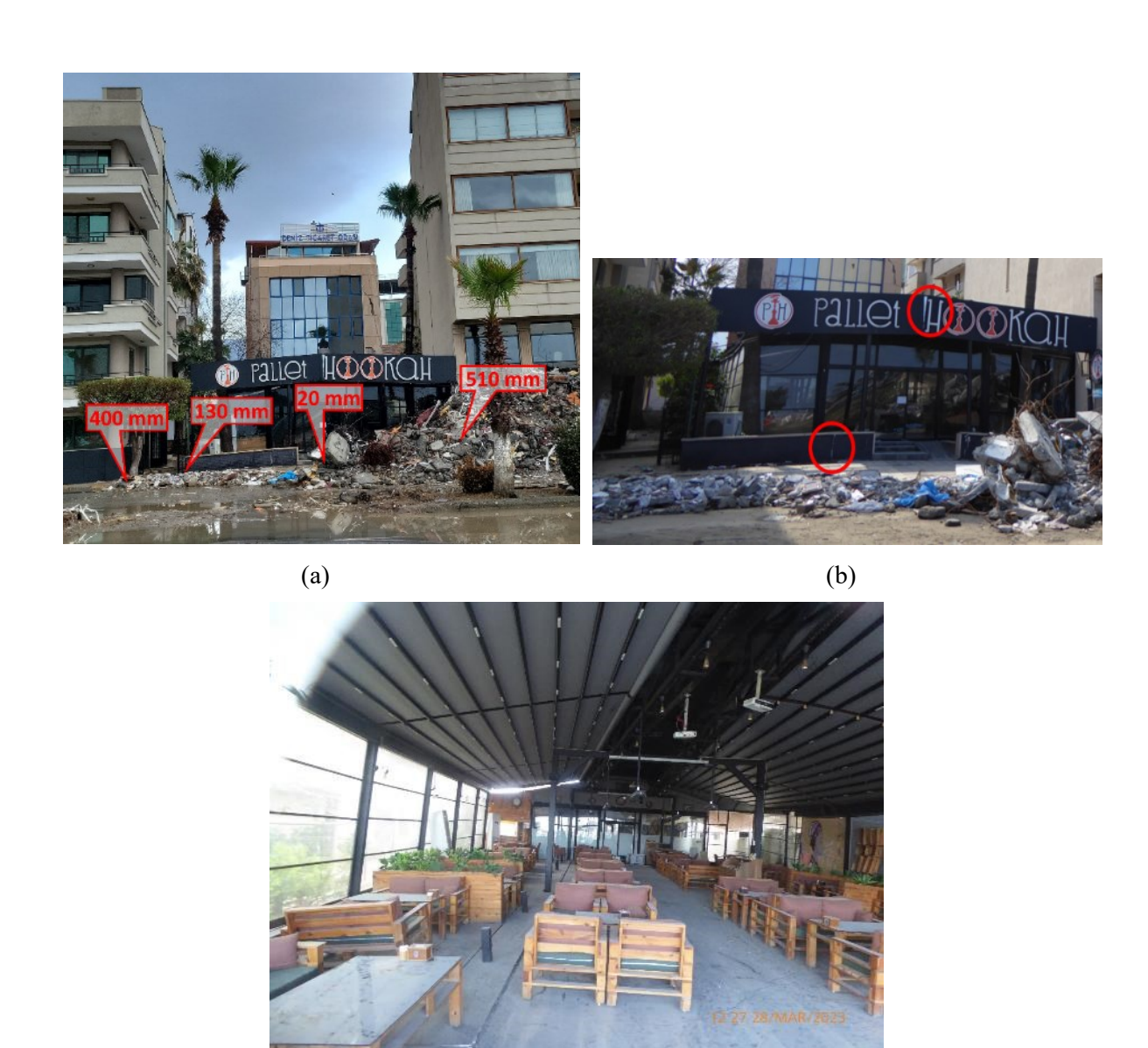


Figure 20. (a) Group of three buildings on Atatürk Boulevard with the restaurant Building L in the middle (36.5909N 36.1777E; 29 MAR 2023), (b) damage to the exterior at Building L associated with hogging ground deformation (36.5906N 36.1778E; 28 MAR 2023), (c) damage to the concrete slab at Building L associated with hogging ground deformation (36.5907N 36.1779E; 28 MAR 2023).

The measured settlements at Building L and the adjacent buildings are plotted with the diamond symbols in Figure 17; note that the error bars on the symbol for settlement at Building K represent uncertainty in the distance between it and Building L. The convex point of the ground deformation is assumed to be the middle of the distance between Buildings K and M. The pattern of ground deformation is similar to the deformations measured in the group of four buildings discussed previously. The consistency of deformation suggests a characteristic pattern for building-ground interactions in this area. Further investigation is required to understand the role of the buildings and subsurface conditions on these ground deformation

patterns. The consistency of measured ground deformation at the Building L restaurant site suggests that the presence of the Building L structure had a minimal influence on the ground deformation between the two heavier buildings.

Sagging Building-Ground Interactions

In contrast to hogging ground deformation, sagging ground deformation is defined by a concave ground curvature. Sagging across a building results in larger settlement beneath the middle of a building relative to the ends of the building. Minor sagging was observed over the footprint of Building W (36.5925N 36.1660E) on Mareşal Fevzi Çakmak Street, which had an average of 60 mm of settlement. The five-story RCF-IW structure is 26.55 m wide and located one block south of Atatürk Boulevard. The middle of the structure had about 10 mm more settlement than both corners. The street view of Building W is pictured in Figure 21a; the building settlement relative to the sidewalk in front of the building is pictured in Figure 21b. Sagging building-ground interactions were also observed across Buildings S, R and Q, as presented previously in Figure 8. Although sagging was not measured for any of these buildings individually, the overall settlement pattern showed larger settlements for the buildings and building corners closest to the center of the city block than for the building corners at the edges of the city block.





Figure 21. Building W on Mareşal Fevzi Çakmak Street: (a) street view of the structure (36.5926N 36.1661E; 28 MAR 2023), and (b) ground and building settlement near the front entrance (36.5926N 36.1661E; 28 MAR 2023).

DISCUSSION

Liquefaction-induced building settlements in Iskenderun were strongly associated with areas of reclaimed land and areas near the historic shoreline with a wide range of settlements measured. Settlements were particularly large in the Çay District, which is entirely founded on reclaimed land. Significant building settlements were documented along the historic shoreline (i.e., Atatürk Boulevard); however, overall building settlements were generally lower than in the Çay District, particularly for five and six-story buildings. While there were observations of ejecta along Atatürk Boulevard outside of the Çay District, ejecta occurrence and amounts were significantly less than those observed in the Çay District, indicating liquefaction was not as prominent along the historic shoreline as in areas of reclaimed land. Historical accounts of the city note that the shoreline was extended beyond Atatürk Boulevard after 1916; satellite imagery and historical maps indicate that reclaimed land in the Çay District was built between 1932 and 1969. Reconnaissance in areas inland from the historic shoreline yielded evidence of moderate or marginal liquefaction or no liquefaction. However, there is some evidence of liquefaction that occurred at depth, including underpass flooding and small building settlements, which did not produce surface evidence of liquefaction.

In the areas of major liquefaction, rigid body tilt of buildings with robust foundations at liquefied sites was observed, as well as one case of a sagging of building foundations for a structure with a more flexible foundation, which is consistent with observations made after other earthquakes (e.g., Bray & Sancio 2009, Bray et al. 2014). Three examples of distinct building-ground interaction were observed. In these cases, the ground appeared to be dragged down by building settlements within a zone of influence around the building; the maximum observed zone of influence was 9.9 m wide. This ground deformation pattern is described as hogging. In one case, a hogging deformation pattern distorted a one-story building (i.e., the Building L restaurant) between two larger nearby buildings.

The ground deformations in the Çay District (group of four buildings and the Building L restaurant) had similar relationships between vertical deformation and distance from the building, as shown in Figure 16. However, the Building T and V settlements and ground deformations do not strictly follow this pattern. The settlements at Buildings T and V were similar to the Çay District mid-rise buildings with the smallest settlements (i.e., Building K and I), however, the distance from Buildings T and V over which the hogging was observed (9.9 m) was larger than at Building K (6.7 m) and Building I (6.25 m). Possible explanations

for the inconsistency include: (a) Buildings T and V are spaced considerably further apart than the buildings where hogging ground deformation was observed in the Çay district, which led to no building-ground-building interaction at Building U, (b) different soil conditions at these sites, and (c) different structural systems and building weights. Further data gathering and research are required to understand the manifestations of hogging ground deformation at liquefaction sites in İskenderun. Understanding the building-ground and building-ground-building interactions is important to identify the conditions that may cause building settlement to induce ground settlement that damages adjacent structures, such as in the Building L restaurant case described in this paper. This is an important consideration in the evaluation of nearby and adjacent buildings with shallow foundations in liquefiable ground.

CONCLUSIONS

Significant liquefaction-induced building settlements were observed in İskenderun, with the most severe liquefaction impacts to buildings occurring in areas of reclaimed land and near historic shorelines. There were cases with negligible settlement (i.e., 0 mm), minor settlement (i.e., < 100 mm), and large settlement (greater than 100 mm and up to 740 mm) documented in these areas. Building-ground interactions were observed where liquefaction-induced building settlement deformed the ground in a notable zone of influence around the building. The observed ground deformation was a dragging down of the ground in a convex pattern called hogging. Three representative cases of this hogging ground deformation between buildings were documented. In one case, free-field conditions existed between the zones of influence from the two buildings; in another case, the zones of influence of building settlement overlapped; and in the third case, the building-induced hogging ground deformations damaged a lightweight building between two heavier buildings.

ACKNOWLEDGEMENTS

GEER Association is supported in part by the National Science Foundation through the Engineering for Civil Infrastructure Program under Grant No. CMMI1826118. Any opinions, findings, conclusions, or recommendations expressed in this material are those of the authors and do not necessarily reflect the views of the NSF. Any use of trade, firm, or product names is for descriptive purposes only and does not imply endorsement by the U.S. Government. The GEER Association is made possible by the vision and support of the NSF Geotechnical Engineering Program Directors: Dr. Giovanna Biscontin, Dr. Richard Fragaszy, and the late

Dr. Cliff Astill. GEER members also donate their time, talent, and resources to collect time-sensitive field observations of the effects of extreme events. Researchers from the Middle East Technical University received support from the Turkish government. Additionally, Zemin Etüd ve Tasarim A.Ş. provided financial support for a team member, and Dr. H. Turan Durgunoğlu provided guidance and logistical support to the team. Dr. Adam Booth (Portland State University) provided the lidar equipment, as well as training on the equipment and data analysis. The team is also grateful for the knowledge and support provided by Dr. Halil Sezen (The Ohio State University), Dr. Ezra Jampole (Exponent), and Dr. Adam Cawood (Southwest Research Institute).

DATA AVAILABILITY

Some or all the data included in this publication are available at Cetin et al. (2023) and Moug et al. (2023) or by reasonable request.

REFERENCES

- Ambraseys, N. N. (1989). Temporary seismic quiescence: S.E. Turkey. *Geophysical Journal International*, 96(2), 311-331.
- Bray, J.D. and Macedo, J. (2017) "6th Ishihara Lecture: Simplified Procedure for Estimating Liquefaction-Induced Building Settlement," *Soil Dynamics and Earthquake Engineering* J., V 102, 215-231, doi: 10.1016/j.soildyn.2017.08.026.
- Bray, J.D. and Sancio, R.B. (2009) "Performance of Buildings in Adapazari during the 1999 Kocaeli, Turkey Earthquake," in *Earthquake Geotechnical Case Histories for Performance Based Design*, Kokusho, T, Ed., TC4 Committee, ISSMFE, CRC Press/Balkema, The Netherlands, 325-340 & Data on CD-ROM.
- Bray, J.D., Cubrinovski, M., Zupan, J., and Taylor, M. (2014) "Liquefaction Effects on Buildings in the Central Business District of Christchurch," *Earthquake Spectra J.*, Earthquake Engineering Research Institute, V 30(1), 85-109, DOI: 10.1193/022113EQS043M.
- Brehme, M., Scheytt, T., Çelik, M., & Dokuz, U. E. (2011). Hydrochemical characterisation of ground and surface water at Dörtyol/Hatay/Turkey. *Environmental Earth Sciences*, *63*, 1395-1408.
- Buckreis, T.E., Pretell, R., Sandikkaya, M.A., Kale, Ö., Askan, A., Brandenberg, S.J., and Stewart, J.P. "February 6, 2023 Türkiye Earthquakes: Ground Motions."

- Cetin, K.Ö., Bray, J.D., Frost, J.D., Hortacsu, A., Miranda, E., Moss, R.E.S., Stewart, J.P. (2023). "February 6, 2023 Turkiye Earthquakes: Report on Geoscience and Engineering Impacts." Earthquake Engineering Research Institute, LFE Program, GEER Association Report 082, May 6, 2023. https://10.18118/G6PM34.
- CloudCompare (version 2.13alpha) [GPL software]. (2023). Retrieved from http://www.cloudcompare.org/
- Maxar Technologies (2023). "Imagery Basemap, Catalog ID: 10300100E1B9D900, Quadkey: 031133021303, Satellite: WV02, Collection date: Feb 12, 2023, 12:16:32-08:00." <maxar.com/open-data/turkey-earthquake-2023>
- Moug, D., Bassal, P., Bray, J.D., Cetin, K.Ö., Kendir, S.B., Sahin, A., Cakir, El., Soylemez,
 B., and Ocak, S. (2023). "February 6, 2023 Türkiye Earthquakes: GEER Phase 3 Team
 Report on Selected Geotechnical Engineering Effects." GEER Association Report 082S1, June 30, 2023. https://doi.org/10.18118/G6F379.
- Nalça, C. (2018). "Transformation of İskenderun Historic Urban Fabric from Mid 19th Century to the End of the French Mandate Period." M.S. Thesis, Department of Architectural Restoration, İzmir Institute of Technology.
- Orukoğlu, N. & İşhani, S. S. (2010). "Hatay Province, İskenderun District, İskenderun Municipality, Microzonation Study Report." Denge Engineering Ltd., Antakya, Turkey.
- Özdemir, A., Yaşar, E., & Şahinoğlu, A. (2019). "Geothermal Geophysical Studies in İskenderun (Hatay): The First Indication for Geothermal Energy." Proceedings of the 3rd International Symposium on Multidisciplinary Studies and Innovative Technologies, Ankara, Turkey.
- SiteEye, Geo-Reconaissance. https://app.sahagozu.com/project/detail/529/viewer/4343. Retrieved August 14, 2023.
- Taftsoglou, M., Valkaniotis, S., Papathanassiou, G., Karantanellis, E. (2023). "Satellite Imagery for Rapid Detection of Liquefaction Surface Manifestations: The Case Study of Türkiye-Syria 2023 Earthquakes. *Remote Sensing*, 15, 4190.
 https://doi.org/10.3390/rs15174190
- Yüce, G., Italiano, F., Yang, F., Yalcin T. H., Fuat Bora, R., Karabacak, V., Gulbay, A.H., Yasin, D.U., Özacar, A. A., D'Alessandro, W., Bellomo, S., Brusca, L., Fu, C., and Lai, C. (2013). "Geochemistry of dissolved and free gases in the Amik Basin (Hatay) and their

relationship with the tectonic structure." Proceedings of the Türkiye Earthquake Engineering and Seismology Conference.